SPECTRAL GAMMA-RAY VARIATIONS OF THE LONG-DURATION FLARE OF 1989 MARCH 6.

H.Marschhäuser, E.Rieger, and G.Kanbach
Max-Planck Institut für Extraterrestrische Physik
D-8046 Garching / Germany

Abstract

We discuss spectral time variations of the flare of March 6, 1989 as the flare progresses from an extremely impulsive phase starting at UT 13:56 to a line-intense gradual phase ending at 14:52. The observations made by the SMM Gamma Ray Spectrometer cover the energy range between 0.3 and 8.5 MeV. We use power law indices, fluences in defined energy bands , hardness ratios and the line intensity of the ^{12}C de-excitation line at 4.438 Mev to reveal the electronic and ionic nature of the radiation. We find that nuclear reactions caused by accelerated protons and ions take place throughout the flare, being most intense at the end. Radiation associated with nuclear processes is however dominated during the impulsive phase by bremsstrahlung of relativistic electrons. These electron dominated spectra show a pronounced hardening above $\sim$ 0.7 MeV deviating from a single power law behavior. During the gradual phase the excess above the power law is dominated by nuclear emissions with evidence for a deviation of the underlying electronic continuum from a simple power law to a steeper behavior .

Introduction As a result of their interaction with the solar atmosphere, flare-accelerated electrons, protons, α-particles and heavier nuclei produce a complex γ-spectrum consisting of a continuum from electron bremsstrahlung and broad and narrow lines from nuclear reactions [1,2]. The narrow lines are produced both by inelastic excitation of heavier nuclei by energetic protons and $\alpha-$particles (direct reactions) and by spallation reactions. The doppler-broadened lines originate from accelerated heavy nuclei losing only a small fraction of their initial kinetic energy after reacting with ambient H or He (inverse reactions). Detector-specific unresolvable lines and broad line components form a "quasi nuclear continuum" in the measured count spectra showing a typical cutoff above $\sim$ 7 Mev. In order to reveal the physical processes involved in particle acceleration, transport and interaction within the flare-loop, it is required to separate the described components. Whereas it is generally accepted to model the dominant electronic part of the radiation $\leq$ 1 MeV with a power law one is left for higher energies with a complicated superposition of unknown continua . To investigate their relative contributions to the spectra of the 1989 March 6 flare we use a model-independent inversion technique.

Observations and Data Analysis The intense X15/3B flare of 6 March, 1989 from active region 5395 was observed by the SMM/GRS for almost 1 h during the total orbital daytime. Fig. 1 shows time histories of the hardest x-ray channel at energies between 110 and 200 keV. Adopting hard x-ray classification the high intensity phases I1 and I2, the minimum phase M1 in between and the transition phase to a lower intensity state T1 correspond to the class of impulsive flares. The following lower intensity phases with variabilities on time scales of minutes are typical for gradual-hard flares. Exact times for the intervals indicated in Fig.1 are given

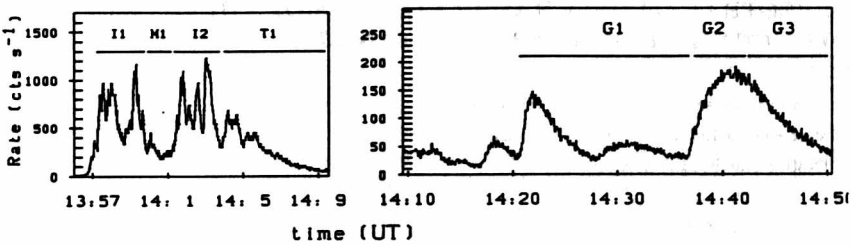

Fig. 1 *Hard x-ray (110-200) keV time histories of the impulsive phases I1, I2, the transition phase T1 and the following gradual phases G1-G3 (see Tab.1).*

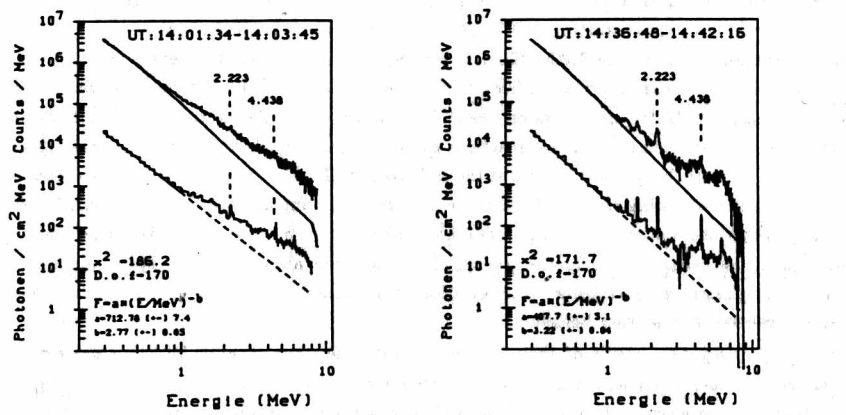

Fig. 2 *Example count spectra (upper curves) and deconvolved photon spectra(lower curves) for phases I2 and G2. The n-capture line (2.223 MeV) and the de-excitation line from ^{12}C (4.438 Mev) are marked. The χ^2 -values give the deviation of the solution in count space from the measured data. F is the fitted differential power law in photon space.*

in Tab.1. The impulsive spikes with variabilities on time scales of seconds show no delay between x-ray and γ-ray emissions (> 10 MeV) within the detector time resolution (2 sec.) [3]. The count spectra in Fig. 2 (upper curves) from phase I2 and G2 are background subtracted and corrected for live time. The lines under these spectra are indicating the detector response to single power law photon spectra obtained by fitting the deconvolved spectra in the energy range $\leq$ 0.7 MeV (lower curves). The data inversion was performed with an iterative numerical procedure searching for a minimum least square solution which utilizes the standard singular value decomposition. To derive the 4.438 MeV line fluence the continuum above 3 MeV was fitted in photon space by gaussians until they passed through all continuum associated 1 σ error intervals. The line intensity was evaluated by fitting the convoluted functional and the detector line response function in count space. A detailed description of the method will be given elsewhere.

Discussion The results of our study are summarized in **Tab.1** and 2. The defined energy bands

Interval $[UT]$	ΔT [s]	index	$\Phi^B_{(0.3-0.8)}$ $[phot./(cm^2 \cdot s)]$	$\Phi^E_{(0.8-2)}$ $[phot./cm^2]$	$\Phi^E_{(4-7)}$ $[phot./cm^2]$
13:57:12-13:59:56 (I1)	163.9	2.49 ± 0.04	20.16 ± 1.32	354.0 ± 22.2	288.3 ± 21.0
13:59:56-14:01:34 (M1)	98.3	2.82 ± 0.05	7.70 ± 0.76	$73.0, \pm 8.2$	26.2 ± 5.7
14:01:34-14:03:45 (I2)	131.1	2.76 ± 0.05	18.50 ± 0.97	238.6 ± 20.3	105.8 ± 12.0
14:04:07-14:10:36 (T1)	409.6	2.96 ± 0.05	6.60 ± 0.55	232.3 ± 20.5	78.5 ± 10.2
14:20:41-14:36:48 (G1)	966.7	3.37 ± 0.04	1.46 ± 0.16	126.9 ± 13.2	75.3 ± 9.6
14:36:48-14:42:18 (G2)	327.7	3.22 ± 0.04	$6.31, \pm 0.43$	75.7 ± 9.8	64.2 ± 7.5
14:42:18-14:50:02 (G3)	458.8	2.98 ± 0.04	5.83 ± 0.39	117.5 ± 13.2	99.5 ± 9.5

Tab.1: Time intervals (see Fig.1), index and continuum quantities of defined energy bands.

	$\Phi_{(4.438)}$	$\Phi^E_{(0.8-2)}/\Phi^E_{(4-7)}$ $[phot./cm^2]$	$\Phi_{(4.438)}/\Phi^E_{(4-7)}$
(I1)	–	1.22 ± 0.12	–
(M1)	< 3	2.79 ± 0.69	< 0.1
(I2)	< 4,	2.25 ± 0.32	< 0.04
(T1)	< 8	2.96 ± 0.46	< 0.1
(G1)	14.6 ± 3.4	1.69 ± 0.28	0.19 ± 0.05
(G2)	12.8 ± 3.6	1.18 ± 0.21	$0.20, \pm 0.06$
(G3)	18.8 ± 3.2	1.18 ± 0.17	0.19 ± 0.04

Tab. 2: 4.438 MeV line fluence, hardness ratios and line to (4-7) MeV continuum.

are choosen to serve as diagnostical quantities to discuss the spectra of the above defined time phases **(Fig. 1)**. Note the given 1 σ errors of the excess take into account both the uncertainties of the power law fit to the limited data sample $\leq 0.7 MeV$ and the errors due to the deconvolution process. $\Phi^B_{(0.3-0.8)}$ gives the flux $[phot./(cm^2 \cdot s)]$ under the power law fit between 0.3 - 0.8 MeV, monitoring the intensity of the bremsstrahlung continuum in this energy range. The power law is used as a line of reference to define the excesses. $\Phi^E_{(.....)}$ are the excess fluences $[phot./cm^2]$. The line fluence $\Phi^L_{(4.438)}$ at 4.438 MeV serves as an independent measure for the nuclear contributions. For pure ionic excesses, $\phi_{(4.438)}/\phi_{(4-7)}$ relates direct and inverse nuclear components depending mainly on the target abundances [6,7]. We find for the different phases: **a) Impulsive phases I1 and I2:** Above about 0.7 MeV a strong spectral hardening can be observed giving rise to an excess continuum extending into the $>$ 10 MeV energy range. Excess values between 7.2 and 8.5 MeV of $\sim$ 40 $phot./cm^2$ (I1) and $\sim$ 10 $phot./cm^2$ (I2) are far above values expected from nuclear emissions. Weak narrow lines are present in I2 (see Fig.2) but dominated by this continuum allowing only to give upper limits for the 4.438 MeV line. This leads to the conclusion that the radiation originates to a great extent from bremsstrahlung of energetic electrons up to the ultra-relativistic regime. The spectra of phase I1 are significantly harder below 0.8 MeV compared to those of I2. The differences of the mean values of Tab.1 differ from zero by 9 σ whereas the $\phi^B_{(0.3-0.8)}$ values are in a comparable range. The difference of the hardness ratios differ from zero by 3 σ giving a confidence level of 99.7 %. The difference is due to a steepening of the bremsstrahlung continuum or/and to a higher relative contribution of nuclear emissions to the excess of I2. **b) Minimum and Transition phases M1 and T1:** The spectra show the typical nuclear continuum variations, but the low upper limits for $\phi_{(4.438)}$ still cannot account for the whole excess as seen from the line-to-continuum ratio $<$ 0.1 (see discussion below). The high hardness ratios of M1 and T1 could reflect the decreased electronic contribution relative to the nuclear component as it might be also the case for phase I2. To verify this a more detailed analysis is needed and subject of our present investigation. The

flattening of the bremsstrahlung continuum obviously takes place in all phases discussed so far. This requires a similar spectral form of the producing electron distribution in momentum space. Observed interplanetary electron spectra associated with impulsive flares show a typical flattening at higher rigidities. [4] explain this flattening by the influence of coulomb losses during stochastic acceleration. Coulomb losses are expected to be important at sites of higher ambient particle densities at lower coronal levels where impulsive flares are thought to occure. The discussed spectra show that protons and ions are accelerated during all phases, however the signature of their γ-radiation is suppressed during I1 and I2. This raises the question whether electrons and ions are accelerated in a common process, prefering electrons during the impulsive phase, or whether there are two independend processes possibly taking place at different sites at the same time.
c) **The gradual-hard phases G1 - G3:** These spectra show very intense nuclear lines (**Fig. 2**). Whereas the line-to-continuum ratios are about equal for all phases the hardness ratios of G2 and G3 display significantly lower values due to exceptional low fluences in the $\phi_{(0.8-2)}$ band. The very intense narrow lines in this energy range from direct nuclear reactions with ambient Ne, Mg, Si and Fe nuclei should produce a much higher nuclear continuum from inverse reactions and unresolvable lines. This contradiction can be due to a gradual steepening of the underlying true electron continuum which would be in this case overestimated by the extrapolated power law fit. This does not significantly change the $\phi_{(4.438)}/\phi_{(4-7)}$ ratios for G1-G3. This is due to the fact that the fluence under the extrapolated power law accounts only for 4% (G1), 10% (G2) and 14% (G3) of the total 4-7 MeV fluence making the $\phi_{(4.438)}/\phi_{(4-7)}$ ratios insensitive to an increase of the power law index. The value of the ratio are slightly below the expected theoretical values between 0.3 and 0.5 derived for different forms of accelarated particle spectra by assuming photospheric abundances and thick target interaction [5]. In a recent abundance study [7] it was found for the 1981 April 27 flare that the ambient gas composition differs from photospheric and coronal compositions. A relative suppression of C from photospheric values as observed in this flare [6] could explain the lower $\phi_{(4.438)}/\phi_{(4-7)}$ ratio of 0.2. To verify this we applied our method to the April 27 flare and found a ratio of 0.17 (+- 0.3) similar to the March 6 event.

Conclusions: Adopting the general picture that γ-rays from impulsive flares originate from the dense regions at deeper sites of the flaring loop and emissions from extended gradual-hard flares from higher coronal levels, the flare of March 6, 1989 offers a unique opportunity to study high energy processes at different loop sites of the same flare. The above study shows that a spectral hardening of the bremsstrahlung continuum around 0.8 MeV takes place during the phases at the beginning of the flare and possibly, a spectral steepening starting below 1 MeV during the gradual end phases. This reveals the important consequence that one has to be very cautious when evaluating nuclear components from single power law approximations of the underlying bremsstrahlung.

References:

1. Ramaty, R. and Lingenfelter.L.E.: 1983, Space Science Rev. **36**, 305.
2. Chupp, E.L., 1984, Ann. Rev. Astron. Astrophys. **22**, 359.
3. Rieger, E. and Marschhäuser H., Proceedings of Max 91 Workshop
4. Steinacker, J., Dröge, W., and Schlickeiser, R.:1988, Solar Phys. **115**,313.
5. Murphy, R.J., 1985, Ph.D. thesis, University of Maryland
6. Forrest, D.J. and Murphy R.J., 1988, Solar Physics **118**,123.
7. Murphy R.J. et al. 1991, Astrophys. J. 371, 793.